

Soft flexural waves and self-localization of wrinkling modes of single- and few-layer graphene under compression in a compliant matrix

Yuriy A. Kosevich *

*N.N. Semenov Federal Research Center for Chemical Physics of Russian Academy of Sciences,
4 Kosygin Street, Moscow 119991, Russia
and Plekhanov Russian University of Economics, Stremyanny pereulok 36, Moscow 117997, Russia*

 (Received 2 April 2021; revised 20 February 2022; accepted 1 March 2022; published 23 March 2022)

This Research Letter studies the evolution under external compression of the wrinkling modes of single- and few-layer graphene or another two-dimensional atomic crystal embedded in or placed on a compliant matrix, or on a dense fluid in a gravitational field. An analytical model based on the nonlinear bending elasticity of the graphene is developed, which shows that the compressive surface stress causes spatial localization of the extended sinusoidal wrinkling mode with a solitonlike envelope, with the localization length decreasing with overcritical external strain. The parameters of the extended sinusoidal wrinkling mode are determined from the conditions of the anomalous softening of the flexural surface acoustic wave with predominant out-of-plane and suppressed in-plane surface displacements, propagating along the graphene in a compliant anisotropic matrix. Self-localization of the wrinkling modes finally results in the formation of strongly localized modes with approximately one-period sinusoidal profiles and external-strain-independent wavelengths. Self-localization of the wrinkling modes is governed by the derived Ginzburg-Landau-type nonlinear envelope-function equation with a negative dispersive term, which we relate with the graphene-nonlinearity-induced repulsion between soft flexural surface acoustic waves with negative effective mass. One- and two-dimensional wrinkling patterns and two types of strongly localized graphene wrinkling modes with different symmetry are described.

DOI: [10.1103/PhysRevB.105.L121408](https://doi.org/10.1103/PhysRevB.105.L121408)

Introduction. The exceptional physical and mechanical properties of graphene have made it very attractive for the construction of nano- and electromechanical devices and as a reinforcing inclusion in polymer nanocomposites [1–5]. As mechanically reinforcing layers in polymer nanocomposites, the graphene layers provide longitudinal stiffness that significantly exceeds the corresponding characteristics of the polymer matrix, which ensures high tensile strength of the nanocomposite in the plane of reinforcement. However, under the compression conditions, the ultimate load of the polymer nanocomposite is determined not only by the strength of its components, including possible nanoparticle fillers [6], but also to a large extent by the loss of stability of the stiff reinforcing layers embedded in the polymer matrix. Primarily, the instability of a uniaxially compressed stiff elastic layer placed on a compliant substrate results in the appearance of an extended sinusoidal wrinkling mode above the critical compressive strain [7–10]. For a stiff elastic layer embedded in a compliant matrix, similar wrinkling instability was first described within the linear macroscopic theory of elasticity [11,12], and with the use of the Winkler model [13,14] and molecular dynamics simulations [15,16] later. In this Research Letter, on the basis of the derived Ginzburg-Landau-type nonlinear envelope-function equation with a negative dispersive term we show that the compressive surface stress in the graphene or another two-dimensional atomic crystal [1,4,5] (such as hexagonal boron nitride), embedded in

or placed on a compliant matrix, or on a dense fluid in a gravitational field, results in spatial localization of the extended sinusoidal wrinkling mode with a solitonlike envelope, with the localization length decreasing with overcritical external strain. We further show that self-localization of the wrinkling modes results finally in the formation of strongly localized modes with approximately one-period sinusoidal profiles and external-strain-independent wavelengths. Both one- and two-dimensional (1D and 2D) wrinkling patterns and two types of strongly localized wrinkling modes with different symmetry are described. The parameters of the extended sinusoidal wrinkling mode are determined from the conditions of anomalous softening of the flexural surface acoustic wave (FSAW) with predominant out-of-plane and suppressed in-plane surface displacements, propagating along the stiff elastic layer embedded in or placed on compliant anisotropic matrix, or on a dense fluid [17–20]. The anomalous softening implies that both the frequency and the group velocity of the FSAW turn to zero at the softening (see Fig. 1), which provides two independent conditions to find out the critical surface stress and the wrinkle wave number and allows us to clarify the origin of the wrinkling modes' self-localization [21].

Localized wrinkling modes (folds with an outward morphology) were observed in glassy polymer film placed on a surface of elastomer substrate [24] and numerically simulated in stiff silicalike film placed on a prestretched nonlinear polymer substrate [25,26], but the elastic properties of both the film and the substrate in these studies are different from those of the graphene and soft linear elastic substrate. The

*yukosevich@gmail.com

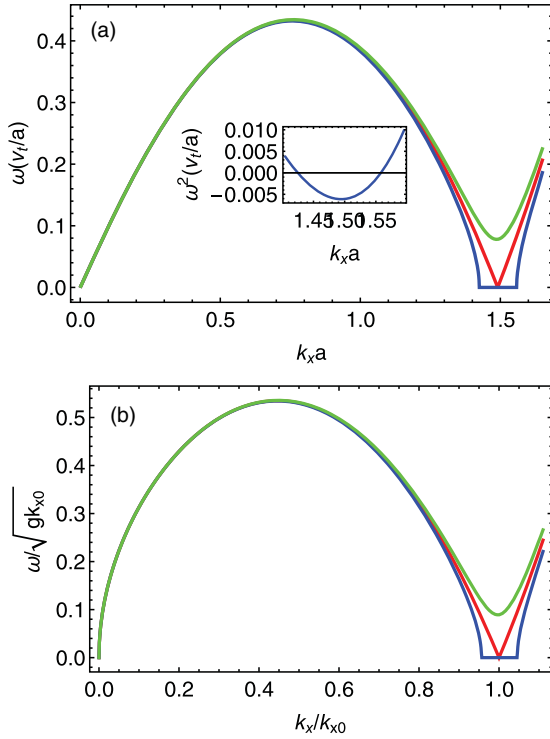


FIG. 1. Anomalous softening of the FSAW, propagating along the graphene monolayer (a) embedded in a matrix of polyethylene or (b) placed on water, caused by compressive strain or negative surface tension. The frequency ω is measured in units (a) of v_t/a , where $v_t = 0.861$ km/s, $a = \rho_s/\rho = 7.6$ Å for the polyethylene with density 998 kg/m³, or (b) of gravity wave frequency $\sqrt{gk_{x0}}$, where $k_{x0} = 4.86 \times 10^5$ m⁻¹; wave number k_x is measured in units (a) of $1/a$ or (b) of k_{x0} . Green, red, and blue lines correspond (a) to the strain $0.998\epsilon_{xx}^{(cr.)}$, $1.0\epsilon_{xx}^{(cr.)}$, and $1.002\epsilon_{xx}^{(cr.)}$ or (b) to the surface tension $0.996G_{xx}^{(cr.)}$, $1.0G_{xx}^{(cr.)}$, and $1.004G_{xx}^{(cr.)}$, respectively. The blue lines show the negative effective mass of the FSAW beyond the softening. The inset in (a) shows ω^2 for the blue line close to $k_{x0} = 1.49/a$, where $\omega^2 < 0$ and the sinusoidal wrinkle with $k_x = k_{x0}$ exponentially grows in time.

localization of subcritical folds was studied in a strut on an elastic foundation [27] and in a thin elastic membrane floating on a dense fluid [28–31], while the proposed model describes the overcritical localization of wrinkling modes in the graphene on a compliant solid matrix or on a dense fluid in a gravitational field. The described overcritical wrinkling with self-localization in the graphene on a dense fluid in a gravitational field [32] is consistent with the observed overcritical buckling with ridge formation in Langmuir monolayers [33–35].

Analytical model and anomalous FSAW softening. The main contributions to the elastic energy of the embedded graphene are given by its in-plane strain $\epsilon_{\alpha\beta}$ produced by (relatively weak) external uniform strain $\epsilon_{\alpha\beta}^0$, and induced out-of-plane $w = u_z^s$ and in-plane u_α^s displacements of the graphene or 2D atomic crystal [36]:

$$\epsilon_{\alpha\beta} = \epsilon_{\alpha\beta}^0 + \frac{1}{2} \left(\frac{\partial u_\alpha^s}{\partial x_\beta} + \frac{\partial u_\beta^s}{\partial x_\alpha} \right) + \frac{1}{2} \frac{\partial w}{\partial x_\alpha} \frac{\partial w}{\partial x_\beta}, \quad (1)$$

when the total static deformation energy of the 2D crystal (isotropic in its plane $z = \text{const}$) can be written in the form

$$E_T = \iint \left\{ \frac{1}{2} \lambda_s \epsilon_{\alpha\alpha}^2 + \mu_s \epsilon_{\alpha\beta}^2 + \frac{1}{2} D_{11} \left(\frac{\partial^2 w}{\partial x^2} + \frac{\partial^2 w}{\partial y^2} \right)^2 + 2D_{66} \left[\left(\frac{\partial^2 w}{\partial x \partial y} \right)^2 - \frac{\partial^2 w}{\partial x^2} \frac{\partial^2 w}{\partial y^2} \right] + \frac{1}{2} K_B(k_x, k_y) w^2 \right\} dx dy, \quad (2)$$

where $\alpha, \beta = 1, 2$; λ_s and μ_s are the 2D Lamé coefficients, which determine the 2D elastic modulus tensor $h_{\alpha\beta\gamma\delta}$; D_{11} and D_{66} , $D_{66} \sim D_{11}$, are the diagonal and torsion bending rigidities of the 2D crystal; and $K_B(k_x, k_y)$ is the positive coefficient, which describes the coupling of the out-of-plane displacement $w(x, y)$ of the 2D crystal with the matrix, assuming the continuity of $w(x, y)$ and corresponding change in the surface-projected bulk stress σ_{zz} at the 2D plane [see Eqs. (3) and (4) below]. Equation (2) implies that nonlinear bending elasticity of the graphene or 2D atomic crystal is determined by the 2D Lamé coefficients λ_s and μ_s and 2D Young's modulus $E_s = h_{11} = \lambda_s + 2\mu_s$, which substantially exceed the corresponding moduli of elasticity of the matrix (multiplied by interatomic distance). This property results in the negligible in-plane in comparison with out-of-plane induced 2D crystal displacements in (2), $u_\alpha^s \ll w$, when the equilibrium bending of the 2D crystal is given by the variational extremum of E_T (2) with respect to $w(x, y)$, $\delta E_T / \delta w = 0$, under the conditions $u_\alpha^s = 0$.

The applicability of the continuum description (2) of graphene wrinkling is determined by the values of the wavelengths of the sinusoidal wrinkling modes, $\lambda_{x0}(n) = 32 \cdot n^{1/3}$ Å and $\lambda_{x0}(n) = 40 \cdot n^{1/3}$ Å, in single- and few-layer graphene, $n = 1, 2, 3, \dots$, embedded in or placed on a polyethylene crystal (Eqs. (S56) and (S57) of the Supplemental Material [32]). These wavelengths are much larger than the carbon-carbon bond length in the graphene layer $a = 1.42$ Å and the interchain spacing in (orthorhombic) polyethylene crystal $r_{\text{min,CC}} \approx 3.8$ Å [37]. Similar conditions for the wrinkle wavelengths should be fulfilled for the possibility of a continuum description of a sheet of another 2D atomic crystal in a compliant matrix.

To find the coefficient K_B in Eq. (2) in the generic case of an anisotropic matrix and find out the origin of the wrinkling modes' self-localization, we turn to the description of anomalous FSAW softening in the system. The long-wavelength elastodynamic properties of the 2D atomic crystal can be taken into account with the use of dynamic boundary conditions for the displacements $u_i^{(1,2)}$ and surface-projected bulk elastic stresses $\sigma_{ni}^{(1,2)}$ in the contacting continuous media 1 and 2 at the plane of the embedded 2D crystal; see, e.g., Refs. [38–40]. The following six linear dynamic boundary conditions are consistent with the deformation energy (2) with $K_B = 0$:

$$u_i^{(1)}(0) = u_i^{(2)}(0) \equiv u_i^s, \quad u_\alpha^s = 0, \quad u_z^s \equiv w, \quad (3)$$

$$\sigma_{nz}^{(1)}(0) - \sigma_{nz}^{(2)}(0) = g_{\alpha\beta} \nabla_\alpha \nabla_\beta w - D_s \Delta_\alpha^2 w - \rho_s \frac{\partial^2 w}{\partial t^2}, \quad (4)$$

where $\sigma_{ni} = \sigma_{ik}n_k$, n_k is a unit vector of the normal to the interface directed from medium 1 into medium 2, $i = 1, 2, 3$, $g_{\alpha\beta} = h_{\alpha\beta\gamma\delta}\epsilon_{\gamma\delta}^0$ is the external-strain-induced surface stress, $D_s = D_{11}$, and ρ_s is the 2D mass density of the layer. More general dynamic boundary conditions, from which Eqs. (3) and (4) and FSAW dispersion equations (S2) and (S4) of the Supplemental Material [32] can be obtained in the limit of very high 2D moduli of elasticity $h_{\alpha\beta\gamma\delta}$ and not very small wave numbers, will be discussed elsewhere.

In the case of uniaxial external compressive strain $\epsilon_{\alpha\beta}^0 = \epsilon_{xx}^0 < 0$, the value of the critical negative surface stress $g_{xx}^{(cr.)} = E_s\epsilon_{xx}^{(cr.)}$ and the wave number k_{x0} , at which the anomalous softening of the FSAW occurs, can be found from the following two conditions [17–20]:

$$\omega(k_{x0}) = 0, \quad \frac{\partial\omega(k_{x0})}{\partial k_x} = 0. \quad (5)$$

In general, we assume the orthorhombic symmetry of the compliant matrix, which can be a polyethylene crystal [37]. With the use of Eqs. (3)–(5) and of Eqs. (S1) and (S2) of the Supplemental Material [32], we find the k_{x0} and critical compressive strain along the [100] direction in the (001) crystal plane:

$$k_{x0} = \left[\frac{B_{\text{bulk,subs}}}{2D_s} \right]^{1/3}, \quad |\epsilon_{xx}^{(cr.)}| = \frac{3D_s^{1/3}}{E_s} \left[\frac{B_{\text{bulk,subs}}}{2} \right]^{2/3}, \quad (6)$$

$$B_{\text{bulk}} = 2B_{\text{subs}} = \frac{2C_{44}C_{33}G}{C_{44} + \sqrt{C_{11}C_{33}}}, \quad (7)$$

$$G = \sqrt{2\sqrt{\frac{C_{11}}{C_{33}} + \frac{C_{11}}{C_{44}} + \frac{C_{44}}{C_{33}} - \frac{(C_{13} + C_{44})^2}{C_{33}C_{44}}}}, \quad (8)$$

where B_{bulk} or B_{subs} is the effective elastic modulus, which determines the parameter $K_B(k_x, k_y) = B|k_{x0}|$ [7] in Eq. (2). As follows from Eqs. (6)–(8), the anisotropic matrix or substrate can result in anisotropy of the wrinkle wave number and critical strain in macroscopically isotropic graphene or 2D atomic crystal under uniaxial strain.

Expressions (7) and (8) are simplified for the isotropic (or transversally isotropic in the xz plane) matrix, when $C_{11} = C_{33}$, $C_{11} - C_{13} = 2C_{44} \equiv 2\mu$, and $G = 2$:

$$B_{\text{bulk}} = 2B_{\text{subs}} = \frac{8\mu(1 - \sigma)}{3 - 4\sigma} = \frac{4E_b(1 - \sigma)}{(1 + \sigma)(3 - 4\sigma)}, \quad (9)$$

where μ , E_b , and σ are the shear modulus, Young's modulus, and Poisson's ratio of the bulk matrix. These values of $B_{\text{bulk,subs}}$ coincide with those obtained from purely static calculations; see, e.g., Refs. [12,41,42]. For the graphene at the interface between two fluids in a gravitational field, the FSAW dispersion, the critical negative surface stress $g_{xx}^{(cr.)}$, and the wave number k_{x0} of the FSAW anomalous softening are given by Eqs. (S6)–(S8) of the Supplemental Material [32].

As follows from Eqs. (6)–(9), the critical compressive strain and wrinkle wave number of the graphene or 2D atomic crystal under compression depend on the substrate moduli of elasticity but do not depend on the parameter of the van der Waals (vdW) interaction between the 2D crystal and substrate (or matrix). As is shown in Ref. [39], in the low-frequency (quasistatic) limit the regime of equal joint out-of-plane

displacements w of the 2D layer and substrate is realized for any nonzero coupling of the layer to the deformable substrate, while the magnitude of such coupling determines the frequencies of the gapped resonances of the physisorbed atoms or graphene sheet on the substrate; see also Refs. [40,43–46]. When applied to the 2D crystal wrinkling, this property leads to the conclusion that the vdW interaction with the deformable substrate determines the threshold for the delamination of the wrinkled 2D crystal from the substrate but does not affect the wrinkling below the delamination threshold, which is considered in this Research Letter.

The origin of self-localization of the extended sinusoidal wrinkling modes we relate with the combination of the repulsive (hard) bending nonlinearity of the graphene or 2D atomic crystal sheet, given by the quartic positive term $(1/8)E_s(\partial w/\partial x)^4$ in Eq. (S9) of the Supplemental Material [32] for 1D patterns and by the term $(1/8)E_s[(\partial w/\partial x)^2 + (\partial w/\partial x)^2]^2$ in Eq. (S31) of the Supplemental Material [32] for 2D patterns, and the *negative effective mass* (NEM) of the soft FSAW, given by the negative inverse second derivative of the FSAW dispersion $(\partial^2\omega/\partial k_x^2)^{-1}$ at $k_x \simeq k_{x0}$ beyond the softening; see the blue lines in Fig. 1 and the Supplemental Material [32] for the parameters of the system. These two features of the considered system result in the effective wrinkle's attraction as a tendency to self-localization. The emergence of the solitonlike envelope of the extended sinusoidal wrinkling mode is similar to the emergence of the envelope solitons and intrinsic localized modes (ILMs or discrete breathers) of the symmetric and antisymmetric type in the Fermi-Pasta-Ulam (FPU) chain with repulsive quartic nonlinearity [47–51], which in the small-amplitude limit are described by the nonlinear Schrödinger equation with hard nonlinearity and negative dispersion, caused by the NEM of short-wavelength acoustic phonons in a monatomic lattice [52,53].

For $|\epsilon_{xx}^0| > |\epsilon_{xx}^{(cr.)}|$, we have $\omega^2(k_{x0}) = -\Gamma^2(k_{x0}) < 0$, and the sinusoidal wrinkles $w \propto \sin(k_x x) \exp[\Gamma(k_x)t]$ grow in time with the maximal growth rate $\Gamma(k_{x0})$ at $k_x = k_{x0}$, which precisely determines the wrinkle wave number k_{x0} [see the inset in Fig. 1(a); the very similar feature in Fig. 1(b) is not shown]. During the exponential growth of w [54], until the saturation imposed by the bending nonlinearity in deformation energy (2) and (S9) in the Supplemental Material [32], the NEM of the soft FSAW and the effective wrinkle's attraction come into play.

1D wrinkling patterns. First we consider the case of one-component external strain in the the x direction, $\epsilon_{\alpha\beta}^0 = \epsilon_{xx}^0 < 0$, when the problem reduces to a 1D one with $w = w(x)$. In our main assumption, the out-of-plane displacement w has the form of a static bending sinusoidal mode with the modulated amplitude, $w = A(x) \sin(k_{x0}x)$. Substituting this ansatz into Eq. (2) with $K_B(k_x, k_y) = B|k_{x0}|$ and averaging over the sinusoidal functions, we get the bending deformation energy per unit area of the 2D atomic crystal E_{def} ; see Eq. (S10) of the Supplemental Material [32]. The equilibrium form $A(x)$ and $k_{x0} > 0$ can be found from the extremum conditions of the bending deformation energy E_{def} with respect to A , $\delta E_{\text{def}}/\delta A = 0$, and k_{x0} , $\partial E_{\text{def}}/\partial k_{x0} = 0$. The latter partial derivative should be taken under the conditions of the unmodulated sinusoidal mode, $A' = A'' = A^{(4)} = 0$, because k_{x0} is the wave number of the extended soft sinusoidal FSAW

with maximal growth rate; see Fig. 1(a) and the Supplemental Material [32]. From the extremum conditions in the weakly modulated limit $|A'| \ll k_{x0}A$, we find the wrinkle wave number $k_{x0} = (B/2D_s)^{1/3}$ and the critical in-plane surface stress and strain, $g_{xx}^{(cr.)} = E_s \epsilon_{xx}^{(cr.)} = -3D_s k_{x0}^2$ (see Eqs. (6)–(8) and Eqs. (S11) and (S12) of the Supplemental Material [32]) and obtain the Ginzburg-Landau-type equation for the external-strain-driven inhomogeneous scalar order parameter $A(x)$,

$$\frac{3}{8}k_{x0}^4 A^3 - (|\epsilon_{xx}^0| - |\epsilon_{xx}^{(cr.)}|)k_{x0}^2 A + (2|\epsilon_{xx}^{(cr.)}| - |\epsilon_{xx}^0|)A'' = 0, \quad (10)$$

in which the dispersive term is negative for weakly overcritical external strain $|\epsilon_{xx}^{(cr.)}| \leq |\epsilon_{xx}^0| < 2|\epsilon_{xx}^{(cr.)}|$. Essentially, the nonlinear envelope-function equation (10) for the 1D pattern and the corresponding equation (15) for the 2D pattern underlie the proposed model of the wrinkle's effective attraction and self-localization: The negative dispersive terms in Eqs. (10) and (15) are the consequence of the NEM of the soft FSAW beyond the softening, which is shown by the blue lines in Fig. 1. The nonlinear envelope-function equation (S24), which is similar to Eq. (10), is also derived for the graphene or 2D atomic crystal placed on a dense fluid in a gravitational field, see Supplemental Material [32].

For the weakly overcritical strain, Eq. (10) describes the two types of self-localized sinusoidal wrinkling modes with the solitonlike envelope, centered at $x = 0$:

$$w_{s,a} = F \frac{(\cos(k_{x0}x), \sin(k_{x0}x))}{\cosh(px)}, \quad (11)$$

$$F = \frac{4}{k_{x0}\sqrt{3}} \sqrt{|\epsilon_{xx}^0| - |\epsilon_{xx}^{(cr.)}|}, \quad (12)$$

$$p = k_{x0} \sqrt{\frac{|\epsilon_{xx}^0| - |\epsilon_{xx}^{(cr.)}|}{2|\epsilon_{xx}^{(cr.)}| - |\epsilon_{xx}^0|}} \ll k_{x0}, \quad (13)$$

where w_s and w_a describe wrinkling modes that are symmetric and antisymmetric in the 2D crystal, respectively. The profile given by $1/\cosh(px)$ in Eq. (11) is typical for 1D solitons in the nonlinear Schrödinger equation [52,55].

As follows from Eqs. (11)–(13), the amplitude F of the broken-symmetry mode increases while the localization length $1/p$ of the solitonlike envelope decreases with the increase in the overcritical external strain $|\epsilon_{xx}^0|$. For large enough $|\epsilon_{xx}^0|$, but still less than $2|\epsilon_{xx}^{(cr.)}|$, when $p \sim k_{x0}$, the modes with solitonlike envelopes (11) transform continuously into strongly localized modes with approximately one-period sinusoidal profiles and external-strain-independent spatial widths; cf. Refs. [50,56,57]. For the symmetric and antisymmetric strongly localized modes, we assume the following ansatz for the profiles:

$$w_{s,a} = (F^{(s)} \cos(k_{x0}^{(s)}x), F^{(a)} \sin(k_{x0}^{(a)}x)) \cos^2(k_{x0}^{(s,a)}x/2), \quad (14)$$

for $-\pi/k_{x0}^{(s,a)} < x < \pi/k_{x0}^{(s,a)}$, and $w = 0$ in the rest of the 2D crystal. Substituting this ansatz into Eq. (2) and assuming the same form of the coefficient $K_B = B^{(s,a)}|k_{x0}^{(s,a)}|$, we find the deformation energy $E_{\text{def}}^{(s,a)}$ as a function of $F^{(s,a)}$ and $k_{x0}^{(s,a)}$ [32]. From the extremum conditions of $E_{\text{def}}^{(s,a)}$ with respect to $F^{(s,a)}$ and $k_{x0}^{(s,a)}$, we obtain the wrinkle wave number

$k_{x0}^{(s,a)} = \kappa^{(s,a)}(B^{(s,a)}/D_s)^{1/3}$, $\kappa^{(s)} = 0.56$, $\kappa^{(a)} = 0.50$; the critical compressive strain $\epsilon_{xx}^{(cr.,s,a)} = \epsilon^{(s,a)}D_s^{1/3}B^{(s,a)2/3}/E_s$, $\epsilon^{(s)} = 2.35$, $\epsilon^{(a)} = 1.88$; and the expression for the localized modes' amplitudes $F^{(s,a)} = (1.89/k_{x0}^{(s,a)})\sqrt{|\epsilon_{xx}^0| - |\epsilon_{xx}^{(cr.,s,a)}|}$ (see Supplemental Material [32]). In the first approximation $B^{(s)} = B^{(a)} = B$, we get $\epsilon_{xx}^{(cr.,s)} = 1.24\epsilon_{xx}^{(cr.,small)}$, $\epsilon_{xx}^{(cr.,a)} = 0.99\epsilon_{xx}^{(cr.,small)}$, where $\epsilon_{xx}^{(cr.,small)}$ is determined in the small-strain limit, described by Eqs. (6)–(8). However, taking into account that $B^{(s,a)} \gtrsim B$ because of the presence of higher spatial harmonics in the profiles (14), we conclude that the transition from the solitonlike envelope to the strongly localized wrinkling modes in the 2D crystal occurs continuously for relatively small overcritical strains, with $|\epsilon_{xx}^{(cr.,small)}| < |\epsilon_{xx}^{(cr.,s,a)}| < 2|\epsilon_{xx}^{(cr.,small)}|$, for which Eqs. (10)–(13) are also valid. This is also clear from the comparison of the profiles of solitonlike solutions (11) with relatively large $p \sim k_{x0}$ with the profiles of strongly localized solutions (14); see Figs. 2(b) and 2(c).

We should underline that the symmetric (antisymmetric) solutions (11) and (14) break (do not break) the *up-down symmetry* of the wrinkling mode. Therefore the antisymmetric modes are presumably realized in the graphene or 2D atomic crystal embedded in the bulk of a compliant matrix when the up-down symmetry is clearly conserved in the defect-free system, while the symmetric modes are realized in the 2D atomic crystal, placed at the crystal-vacuum interface or on a dense fluid in a gravitational field. In the former case, the outward morphology of the symmetric wrinkling mode is governed by the additional weak nonlinear cubic term in Eq. (2), $\propto (-k_{x0}^2 w^3)$, which is provided by the nonlinear solid substrate with realistic interatomic potentials that are softer for the outward than for the inward surface displacements. In the latter case, the inward direction of the symmetric sheet deformation is determined by the term $\rho_s g w$ in Eq. (S18) due to the gravitational field, which does not enter the extremum conditions for the wrinkling of the infinite sheet [28,32]. These conclusions, together with the displacement profiles and symmetry of the wrinkling modes shown in Figs. 2(a)–2(c), are consistent with the observation in recent molecular dynamics simulations of the outward symmetric (antisymmetric) wrinkling of a graphene nanoribbon under compression placed on (in) a polyethylene crystal [58]. Significantly, due to the lack of delamination the strongly localized antisymmetric wrinkling modes in the embedded graphene or 2D atomic crystal are not equivalent to the ripplocations in layered solids [59,60].

It is important to emphasize that the proposed model of wrinkling modes' localization in 2D atomic crystal is based on the assumption that the repulsive quartic nonlinear term $(1/8)E_s(\partial w/\partial x)^4$ in Eq. (S9) and the term $(1/8)E_s[(\partial w/\partial x)^2 + (\partial w/\partial x)^2]^2$ in Eq. (S30) of the Supplemental Material [32] are larger than the aforementioned cubic nonlinear term, $\propto (-k_{x0}^2 w^3)$, provided by the substrate, because of the very high 2D Young's modulus E_s of the 2D atomic crystal, graphene first of all, in comparison with the moduli of elasticity of the compliant substrate (multiplied by the interatomic distance). The proposed model does not include the period-doubling bifurcation in the wrinkling morphology that was described in the model of wrinkle focalization in a linear stiff polymer membrane on a nonlinear

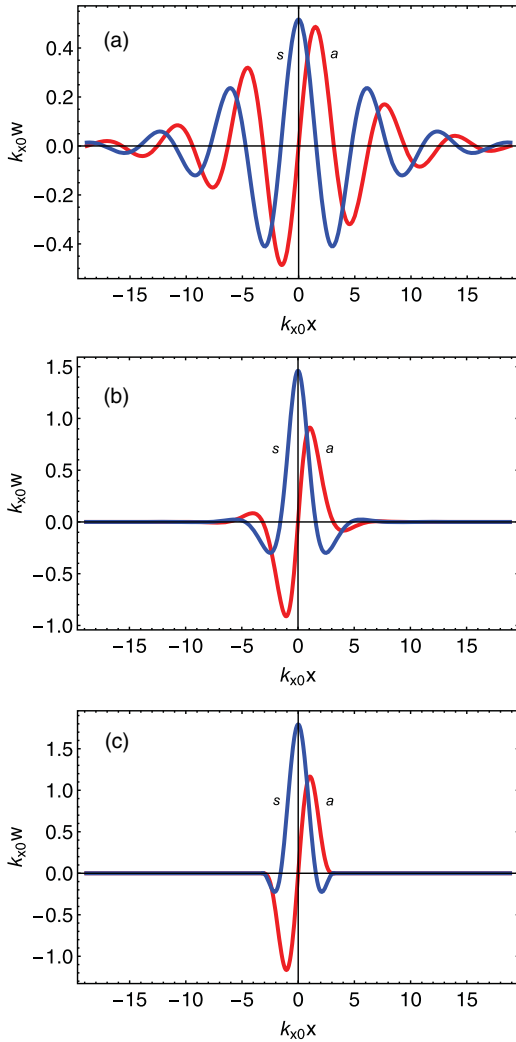


FIG. 2. Normalized by $\sqrt{|\epsilon_{xx}^{(cr.)}|}$ displacement profiles of symmetric “s” and antisymmetric “a” wrinkling modes with solitonlike envelopes (11), for (a) $|\epsilon_{xx}^0| = 1.05|\epsilon_{xx}^{(cr.)}|$ and (b) $|\epsilon_{xx}^0| = 1.4|\epsilon_{xx}^{(cr.)}|$, and of strongly localized modes (14) for (c) $|\epsilon_{xx}^0| = 1.9|\epsilon_{xx}^{(cr.)}|$. Profiles of the symmetric wrinkling modes correspond to outward or inward deflection of the graphene or 2D atomic crystal placed on soft solid substrate or on dense fluid in a gravitational field, respectively.

elastomer substrate in Ref. [61], which is based on the opposite assumption of the dominance of the nonlinear cubic term over the quartic one in the considered system. It is also worth noting that ILMs can exist in FPU lattices only with a relatively small cubic term in comparison with the repulsive quartic term in the interatomic potential [47], and the existence of ILMs in such lattices is not related with the period-doubling instability of the zone-boundary mode [62]. These facts provide yet another piece of evidence for the similarity of the nonlinear governing potentials and of the necessary condition for the existence of self-localized wrinkling modes in 2D atomic crystals and of ILMs in FPU lattices: the dominance of the repulsive quartic nonlinearity in the corresponding system.

For the graphene or 2D atomic crystal with n layers, when both $D_s(n)$ and $E_s(n)$ increasing with n , Eqs. (6)–(8) pre-

dict the decrease with n in the wrinkle wave number k_{x0} and modulus of the critical compressive strain $|\epsilon_{xx}^{(cr.)}|$ [14,20], which demonstrates the non-Eulerian nature of the bending instability of the 2D elastic layer embedded in or placed on a compliant matrix [14]. In the case of weak interlayer coupling in the few-layer graphene or 2D atomic crystal, the individual layers are prone to relative sliding, and the bending stiffness of the multilayer $D_s(n)$ can be taken as a sum of the bending stiffnesses of each layer $D_s(1)$ [14,20,63,64], $D_s(n) = nD_s(1)$, and $E_s(n) = nE_s(1)$, when Eqs. (6)–(8) predict $k_{x0} \propto n^{-1/3}$ and $|\epsilon_{xx}^{(cr.)}| \propto n^{-2/3}$; see Supplemental Material [32].

2D wrinkling patterns. First we consider the case of the *equibiaxial* external compressive strain $\epsilon_{xx}^0 = \epsilon_{yy}^0 < 0$, which results in $g_{xx} = g_{yy} < 0$, when the extended checkerboard wrinkling mode is realized for weak overcritical strain with $w = A \sin(\kappa_{x0}x) \sin(\kappa_{y0}y)$, $\kappa_{x0} = \kappa_{y0}$; see, e.g., Refs. [65,66]. It is worth noting that the equibiaxial compressive strain can also be realized by cooling the system of graphene or another hexagonal 2D atomic crystal embedded in or placed on a soft isotropic matrix. The dispersion equations of the FSAW with three-component displacement fields in this case are given by Eqs. (S3) and (S4) of the Supplemental Material [32]. From the conditions of the anomalous FSAW softening (5) for $\omega(\kappa_x)$ given by Eqs. (S3) and (S4), we get the wrinkle wave

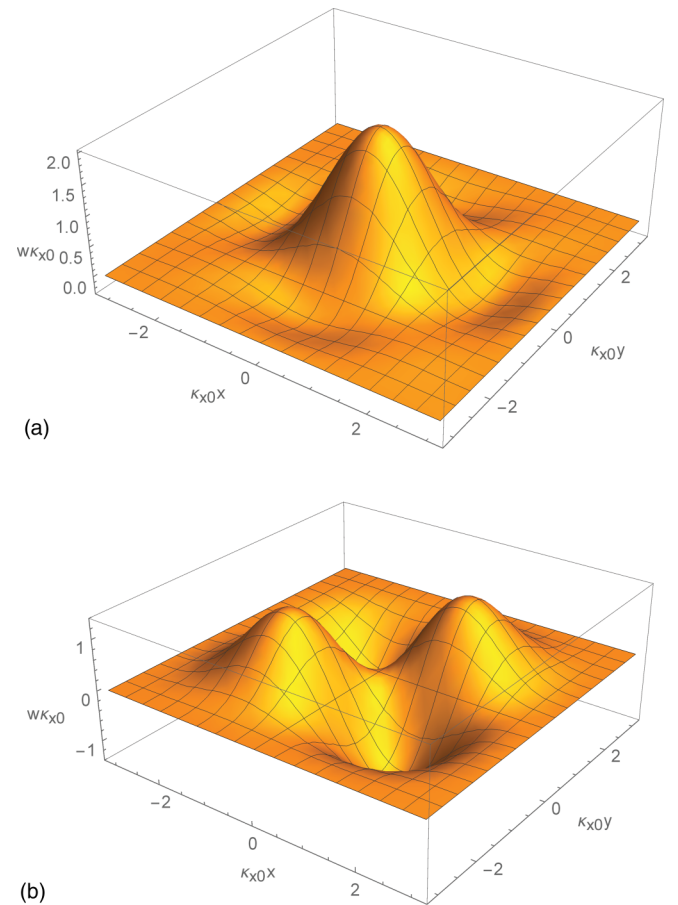


FIG. 3. Normalized by $\sqrt{|g_{xx}^{(cr.)}|/h_{11}}$ displacement profiles of (a) symmetric and (b) antisymmetric strongly localized wrinkling modes in 2D patterns for overcritical equibiaxial external compressive surface stress.

number $\kappa_{x0} = k_{x0}/\sqrt{2}$ [65] and the critical in-plane surface stress and strain $g_{xx}^{(cr.)} = (h_{11} + h_{12})\epsilon_{xx}^{(cr.2D)} = h_{11}\epsilon_{xx}^{(cr.1D)} = -6D_s\kappa_{x0}^2$, $\epsilon_{xx}^{(cr.2D)} = \epsilon_{yy}^{(cr.2D)}$, where k_{x0} and $\epsilon_{xx}^{(cr.1D)}$ are the corresponding parameters in the 1D wrinkling pattern, Eq. (6). These parameters enter the Ginzburg-Landau-type equation for the envelope $A(x, y)$ of the modulated checkerboard wrinkling mode in 2D patterns [32],

$$\frac{1}{32}(10h_{11} - h_{66})\kappa_{x0}^4 A^3 - (|g_{xx}| - |g_{xx}^{(cr.)}|)\kappa_{x0}^2 A + \frac{1}{2}\left(\frac{4}{3}|g_{xx}^{(cr.)}| - |g_{xx}|\right)(A_{,xx} + A_{,yy}) = 0, \quad (15)$$

in which the dispersive term is negative for weakly overcritical surface stress $|g_{xx}^{(cr.)}| < |g_{xx}| < (4/3)|g_{xx}^{(cr.)}|$. Since Eq. (15) does not have a simple analytical solution, we describe the ansatz for the symmetric and antisymmetric strongly localized wrinkling modes in 2D patterns; see Eqs. (S38)–(S45) of the Supplemental Material [32] and Figs. 3(a) and 3(b) for the normalized profiles of two types of strongly localized wrinkling modes in 2D patterns for overcritical equibiaxial external compressive surface stress.

We also consider the case of the radial and polar cylindrically-symmetrical external compressive strain $\epsilon_{rr}^0 = \epsilon_{\phi\phi}^0 = \text{const} < 0$, applied to the circular graphene or 2D

atomic crystal sheet embedded in or placed on a cylindrical soft matrix. The corresponding symmetric and antisymmetric strongly localized wrinkling modes are described by the combinations of the Bessel and modified Bessel functions of the radial coordinate and are confined in the circular areas of the radius $r_{\text{loc}}^{(s,a)} \sim 6/\kappa_{x0}^{(s,a)}$ with effectively “clamped” edges; see Eqs. (S50) and (S51) and Fig. S1 of the Supplemental Material [32].

In summary, we demonstrate with an analytical model the phenomenon of self-localization of the sinusoidal wrinkling mode of single- and few-layer graphene or another 2D atomic crystal under compression, embedded in or placed on a compliant matrix, or on a dense fluid in a gravitational field. Self-localization is caused by hard bending nonlinearity of the 2D crystal and negative effective mass of the soft FSAW beyond the softening, and results in the formation of strongly localized wrinkling modes with approximately one-period sinusoidal profiles and strain-independent wavelengths. The presented results can be important for possible applications in flexible electronics and mechatronics.

Acknowledgments. The author is grateful to S. Bazhenov, A. V. Savin, and I. A. Strelnikov for useful discussions. This work was supported by the Russian Foundation for Basic Research (Project No. 18-29-19135).

-
- [1] K. S. Novoselov, D. Jiang, F. Schedin, T. J. Booth, V. V. Khotkevich, S. V. Morozov, and A. K. Geim, Two-dimensional atomic crystals, *Proc. Natl. Acad. Sci. USA* **102**, 10451 (2005).
- [2] A. K. Geim and K. S. Novoselov, The rise of graphene, *Nat. Mater.* **6**, 183 (2007).
- [3] C. Lee, X. Wei, J. W. Kysar, and J. Hone, Measurement of the elastic properties and intrinsic strength of monolayer graphene, *Science* **321**, 385 (2008).
- [4] D. Akinwande, C. J. Brennan, J. S. Bunch, P. Egberts, J. R. Felts, H. Gao, R. Huang, J.-S. Kim, T. Li, Y. Li, K. M. Liechti, N. Lu, H. S. Park, E. J. Reed, P. Wang, B. I. Yakobson, T. Zhang, Y.-W. Zhang, Y. Zhou, and Y. Zhu, A review on mechanics and mechanical properties of 2D materials—Graphene and beyond, *Extreme Mech. Lett.* **13**, 42 (2017).
- [5] R. Roldán, L. Chirrolli, E. Prada, J. A. Silva-Guillén, P. San-Jose, and F. Guinea, Theory of 2D crystals: graphene and beyond, *Chem. Soc. Rev.* **46**, 4387 (2017).
- [6] R. Sun, M. Melton, N. Safaie, R. C. Ferrier, Jr., S. Cheng, Y. Liu, X. Zuo, and Y. Wang, Molecular View on Mechanical Reinforcement in Polymer Nanocomposites, *Phys. Rev. Lett.* **126**, 117801 (2021).
- [7] M. A. Biot, Bending of an infinite beam on an elastic foundation, *J. Appl. Mech.* **59**, A1 (1937).
- [8] N. Bowden, S. Brittain, A. G. Evans, J. W. Hutchinson, and G. M. Whitesides, Spontaneous formation of ordered structures in thin films of metals supported on an elastomeric polymer, *Nature (London)* **393**, 146 (1998).
- [9] A. L. Volynskii, S. Bazhenov, O. V. Lebedeva, and N. F. Bakeev, Mechanical buckling instability of thin coatings deposited on soft polymer substrates, *J. Mater. Sci.* **35**, 547 (2000).
- [10] W. Huck, N. Bowden, P. Onck, T. Pardo, J. W. Hutchinson, and G. M. Whitesides, Ordering of spontaneously formed buckles on planar surfaces, *Langmuir* **16**, 3497 (2000).
- [11] M. A. Biot, Folding instability of a layered viscoelastic medium under compression, *Proc. R. Soc. London, Ser. A* **242**, 444 (1957).
- [12] H. J. Allen, *Analysis and Design of Structural Sandwich Panels* (Pergamon Press, Oxford, 1969).
- [13] Ch. Androulidakis, E. N. Koukaras, O. Frank, G. Tsoukleri, D. Sfyris, J. Parthenios, N. Pugno, K. Papagelis, K. S. Novoselov, and C. Galiotis, Failure processes in embedded monolayer graphene under axial compression, *Sci. Rep.* **4**, 5271 (2014).
- [14] Ch. Androulidakis, E. N. Koukaras, M. Hadjinicolaou, and C. Galiotis, Non-Eulerian behavior of graphitic materials under compression, *Carbon* **138**, 227 (2018).
- [15] F. Lin, Y. Xiang, and H.-S. Shen, Buckling of graphene embedded in polymer matrix under compression, *Int. J. Struct. Stab. Dyn.* **15**, 1540016 (2015).
- [16] E. N. Koukaras, C. Androulidakis, G. Anagnostopoulos, K. Papagelis, and C. Galiotis, Compression behavior of simply-supported and fully embedded monolayer graphene: Theory and experiment, *Extreme Mech. Lett.* **8**, 191 (2016).
- [17] Yu. A. Kosevich and E. S. Syркин, Capillary phenomena and elastic waves localized near a plane crystal defect, *Phys. Lett. A* **122**, 178 (1987).
- [18] Yu. A. Kosevich and E. S. Syркин, Anomalies of surface elastic waves and the formation of superstructures during two-dimensional deformation transitions, *Solid State Phys.* **29**, 3174 (1987) (in Russian).
- [19] Yu. A. Kosevich, L. G. Potyomina, A. N. Darinskii, and I. A. Strelnikov, Phonon interference control of atomic-scale metamirrors, meta-absorbers, and heat transfer through crystal interfaces, *Phys. Rev. B* **97**, 094117 (2018).

- [20] Yu. A. Kosevich, A. A. Kistanov, and I. A. Strelnikov, Bending instability of few-layer graphene embedded in strained polymer matrix, *Lett. Mater.* **8**, 278 (2018).
- [21] It is worth noting that the conditions for zeroing the frequency and group velocity of density waves and the hard-nonlinearity-based approach can also be used in the study of gravitational instability in a rotating self-gravitating disk and modeling the formation of spiral galaxies [22] and Saturn's rings [23].
- [22] A. Toomre, Group velocity of spiral waves in galactic disks, *Astrophys. J.* **158**, 899 (1969).
- [23] A. M. Fridman and V. L. Polyachenko, *Physics of Gravitating Systems II. Nonlinear Collective Processes: Nonlinear Waves, Solitons, Collisionless Shocks, Turbulence. Astrophysical Applications* (Springer, New York, 1984).
- [24] Y. Ebata, A. B. Croll, and A. J. Crosby, Wrinkling and strain localizations in polymer thin films, *Soft Matter* **8**, 9086 (2012).
- [25] Y. Cao and J. W. Hutchinson, Wrinkling phenomena in neo-Hookean film/substrate systems, *J. Appl. Mech.* **79**, 031019 (2012).
- [26] J. Zang, X. Zhang, Y. Cao, and J. W. Hutchinson, Localized ridge wrinkling of stiff films on compliant substrates, *J. Mech. Phys. Solids* **60**, 1265 (2012).
- [27] G. W. Hunt, M. K. Wadee, and N. Shiacolas, Localized elasticae for the strut on the linear foundation, *J. Appl. Mech.* **60**, 1033 (1993).
- [28] L. Pocivavsek, R. Dellsy, A. Kern, S. Johnson, B. Lin, K. Y. C. Lee, and E. Cerda, Stress and fold localization in thin elastic membranes, *Science* **320**, 912 (2008).
- [29] H. Diamant and T. A. Witten, Instability of infinitesimal wrinkles against folding, [arXiv:1009.2487v2](https://arxiv.org/abs/1009.2487v2).
- [30] B. Audoly, Localized buckling of a floating elastica, *Phys. Rev. E* **84**, 011605 (2011).
- [31] H. Diamant and T. A. Witten, Compression Induced Folding of a Sheet: An Integrable System, *Phys. Rev. Lett.* **107**, 164302 (2011).
- [32] See Supplemental Material at <http://link.aps.org/supplemental/10.1103/PhysRevB.105.L121408> for a more detailed description of the dispersion equations of the FSAW propagating along the graphene or 2D atomic crystal embedded in or placed on a soft orthorhombic matrix or on a dense fluid in a gravitational field, the general form of the nonlinear envelope-function equations in 1D and 2D wrinkling patterns, a more detailed description of strongly localized wrinkling modes in 1D and 2D wrinkling patterns, and the parameters of the graphene and soft polyethylene matrix that realize the anomalous softening of the FSAW shown in Figs. 1(a) and 1(b). This includes Refs. [67–78].
- [33] H. E. Ries Jr., Stable ridges in a collapsing monolayer, *Nature (London)* **281**, 287 (1979).
- [34] S. T. Milner, J.-F. Joanny, and P. Pincus, Buckling of Langmuir monolayers, *Europhys. Lett.* **9**, 495 (1989).
- [35] W. Lu, C. M. Knobler, R. F. Bruinsma, M. Twardos, and M. Dennin, Folding Langmuir Monolayers, *Phys. Rev. Lett.* **89**, 146107 (2002).
- [36] L. D. Landau, E. M. Lifshitz, A. M. Kosevich, and L. P. Pitaevskii, *Theory of Elasticity*, 3rd ed. (Pergamon Press, Oxford, 1986).
- [37] I. A. Strelnikov and E. A. Zubova, Shear-induced martensitic transformations in crystalline polyethylene: Direct molecular-dynamics simulations, *Phys. Rev. B* **99**, 134104 (2019).
- [38] A. F. Andreev and Yu. A. Kosevich, Capillary phenomena in the theory of elasticity, *Zh. Eksp. Teor. Fiz.* **81**, 1435 (1981) [*JETP* **54**, 761 (1981)].
- [39] Yu. A. Kosevich and E. S. Syrkin, Long wavelength surface oscillations of a crystal with an adsorbed monolayer, *Phys. Lett. A* **135**, 298 (1989).
- [40] Yu. A. Kosevich, Capillary phenomena and macroscopic dynamics of complex two-dimensional defects in crystals, *Prog. Surf. Sci.* **55**, 1 (1997).
- [41] J. Groenewold, Wrinkling of plates coupled with soft elastic media, *Phys. A (Amsterdam)* **298**, 32 (2001).
- [42] B. Audoly and A. Boudaoud, Buckling of a thin film bound to a compliant substrate—Part I: formulation, linear stability of cylindrical patterns, secondary bifurcations, *J. Mech. Phys. Solids* **56**, 2401 (2008).
- [43] E. A. Garova, A. A. Maradudin, and A. P. Mayer, Interaction of Rayleigh waves with randomly distributed oscillators on the surface, *Phys. Rev. B* **59**, 13291 (1999).
- [44] N. Boechler, J. K. Eliason, A. Kumar, A. A. Maznev, K. A. Nelson, and N. Fang, Interaction of a Contact Resonance of Microspheres with Surface Acoustic Waves, *Phys. Rev. Lett.* **111**, 036103 (2013).
- [45] Y. Ni, Yu. A. Kosevich, S. Xiong, Y. Chalopin, and S. Volz, Substrate-induced cross-plane thermal propagative modes in few-layer graphene, *Phys. Rev. B* **89**, 205413 (2014).
- [46] A. A. Maznev and V. E. Gusev, Waveguiding by a locally resonant metasurface, *Phys. Rev. B* **92**, 115422 (2015).
- [47] A. M. Kosevich and A. S. Kovalev, Self-localization of vibrations in a one-dimensional anharmonic chain, *Zh. Eksp. Teor. Fiz.* **67**, 1793 (1974) [*JETP* **40**, 891 (1975)].
- [48] A. J. Sievers and S. Takeno, Intrinsic Localized Modes in Anharmonic Crystals, *Phys. Rev. Lett.* **61**, 970 (1988).
- [49] J. B. Page, Asymptotic solutions for localized vibrational modes in strongly anharmonic periodic systems, *Phys. Rev. B* **41**, 7835 (1990).
- [50] Yu. A. Kosevich, Nonlinear envelope-function equation and strongly localized vibrational modes in anharmonic lattices, *Phys. Rev. B* **47**, 3138 (1993).
- [51] S. Flach and C. R. Willis, Discrete breathers, *Phys. Rep.* **295**, 181 (1998).
- [52] Yu. A. Kosevich and S. Lepri, Modulational instability and energy localization in anharmonic lattices at finite energy density, *Phys. Rev. B* **61**, 299 (2000).
- [53] Yu. A. Kosevich, Charged ultradiscrete supersonic kinks and discrete breathers in nonlinear molecular chains with realistic interatomic potentials and electron-phonon interactions, *J. Phys.: Conf. Ser.* **833**, 012021 (2017).
- [54] F. Box, O. Kodio, D. O'Kiely, V. Cantelli, A. Goriely, and D. Vella, Dynamic Buckling of an Elastic Ring in a Soap Film, *Phys. Rev. Lett.* **124**, 198003 (2020).
- [55] C. Sulem and P.-L. Sulem, *The Nonlinear Schrödinger Equation. Self-Focusing and Wave Collapse* (Springer, New York, 1999).
- [56] Yu. A. Kosevich, Nonlinear Sinusoidal Waves and Their Superposition in Anharmonic lattices, *Phys. Rev. Lett.* **71**, 2058 (1993).
- [57] Yu. A. Kosevich, R. Khomeriki, and S. Ruffo, Supersonic discrete kink-solitons and sinusoidal patterns with “magic” wave number in anharmonic lattices, *Europhys. Lett.* **66**, 21 (2004).

- [58] A. V. Savin, 2D model graphene nanoribbons in a polymer matrix, *Polym. Sci. Ser. A* **63**, 344 (2021).
- [59] A. Kushima, X. Qian, P. Zhao, S. Zhang, and J. Li, Ripplifications in van der Waals layers, *Nano Lett.* **15**, 1302 (2015).
- [60] M. W. Barsoum, Ripplifications: A progress report, *Front. Mater.* **7**, 146 (2020).
- [61] F. Brau, H. Vandeparre, A. Sabbah, C. Poulard, A. Boudaoud, and P. Damman, Multiple-length-scale elastic instability mimics parametric resonance of nonlinear oscillators, *Nat Phys.* **7**, 56 (2011).
- [62] K. W. Sandusky and J. B. Page, Interrelation between the stability of extended normal modes and the existence of intrinsic localized modes in nonlinear lattices with realistic potentials, *Phys. Rev. B* **50**, 866 (1994).
- [63] K. V. Zakharchenko, J. H. Los, M. I. Katsnelson, and A. Fasolino, Atomistic simulations of structural and thermodynamic properties of bilayer graphene, *Phys. Rev. B* **81**, 235439 (2010).
- [64] D.-M. Tang, D. G. Kvashnin, S. Najmaei, Y. Bando, K. Kimoto, P. Koskinen, P. M. Ajayan, B. I. Yakobson, P. B. Sorokin, J. Lou, and D. Golberg, Nanomechanical cleavage of molybdenum disulphide atomic layers, *Nat. Commun.* **5**, 3631 (2014).
- [65] X. Chen and J. W. Hutchinson, A family of herringbone patterns in thin films, *Scr. Mater.* **50**, 797 (2004).
- [66] J. Song, H. Jiang, W. M. Choi, D. Y. Khang, Y. Huang, and J. A. Rogers, An analytical study of two-dimensional buckling of thin films on compliant substrates, *J. Appl. Phys. (Melville, NY)* **103**, 014303 (2008).
- [67] Yu. A. Kosevich and E. S. Syrkin, Existence criterion and properties of deeply penetrating Rayleigh waves in crystals, *Zh. Eksp. Teor. Fiz.* **89**, 2221 (1985) [*JETP* **62**, 1282 (1985)].
- [68] Yu. A. Kosevich and E. S. Syrkin, Collective oscillations of twin boundaries in high-temperature superconductors as an acoustic analogue of two-dimensional plasmons, *Phys. Rev. B* **43**, 326 (1991).
- [69] L. D. Landau and E. M. Lifshitz, *Fluid Mechanics* (Pergamon Press, New York, 1987).
- [70] R. Y. Chiao, E. Garmire, and C. H. Townes, Self-trapping of Optical Beams, *Phys. Rev. Lett.* **13**, 479 (1964).
- [71] K. E. Graff, *Wave Motion in Elastic Solids* (Clarendon Press, Oxford, 1975).
- [72] T. J. Booth, P. Blake, R. R. Nair, Da Jiang, E. W. Hill, U. Bangert, A. Bleloch, M. Gass, K. S. Novoselov, M. I. Katsnelson, and A. K. Geim, Macroscopic graphene membranes and their extraordinary stiffness, *Nano Lett.* **8**, 2442 (2008).
- [73] A. Fasolino, J. H. Los, and M. I. Katsnelson, Intrinsic ripples in graphene, *Nat. Mater.* **6**, 858 (2007).
- [74] A. H. Castro Neto, F. Guinea, N. M. R. Peres, K. S. Novoselov, and A. K. Geim, The electronic properties of graphene, *Rev. Mod. Phys.* **81**, 109 (2009).
- [75] R. Nicklow, N. Wakabayashi, and H. G. Smith, Lattice dynamics of pyrolytic graphite, *Phys. Rev. B* **5**, 4951 (1972).
- [76] O. L. Blakslee, D. G. Proctor, E. J. Seldin, G. B. Spence, and T. Weng, Elastic constants of compression-annealed pyrolytic graphite, *J. Appl. Phys. (Melville, NY)* **41**, 3373 (1970).
- [77] Y. W. Sun, W. Liu, I. Hernandez, J. Gonzalez, F. Rodriguez, D. J. Dunstan, and C. J. Humphreys, 3D Strain in 2D Materials: To What Extent is Monolayer Graphene Graphite? *Phys. Rev. Lett.* **123**, 135501 (2019).
- [78] W. Paul and D. Y. Yoon, An optimized united atom model for simulations of polymethylene melts, *J. Chem. Phys.* **103**, 1702 (1995).